Article

1,4,5,8,9,12-Hexamethyltriphenylene. A Molecule with a Flipping Twist

Yi Wang, Andrew D Stretton, Mark C McConnell, Peter A. Wood,
Simon Parsons, John B Henry, Andrew R Mount, and Trent H Galow

J. Am. Chem. Soc., **2007**, 129 (43), 13193-13200• DOI: 10.1021/ja074120j • Publication Date (Web): 06 October 2007

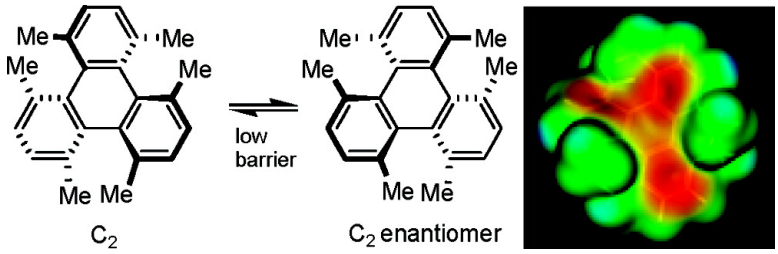

More About This Article

Additional resources and features associated with this article are available within the HTML version:

- Supporting Information
- Links to the 2 articles that cite this article, as of the time of this article download
- Access to high resolution figures
- Links to articles and content related to this article
- Copyright permission to reproduce figures and/or text from this article

View the Full Text HTML

J|A|C|S
ARTICLES
Published on Web 10/06/2007

1,4,5,8,9,12-Hexamethyltriphenylene. A Molecule with a Flipping Twist

Yi Wang, Andrew D Stretton, Mark C McConnell, Peter A. Wood, Simon Parsons, John B Henry, Andrew R Mount,* and Trent H Galow*

Contribution from the School of Chemistry, University of Edinburgh, The King's Buildings, West Mains Road, Edinburgh EH9 3JJ, U.K.

Received June 6, 2007; E-mail: trent.galow@ed.ac.uk

Abstract: The synthesis and characterization of 1,4,5,8,9,12-hexamethyltriphenylene (**5**) is described. In the solid state, X-ray crystallographic studies reveal that compound **5** presents a highly distorted C_2 geometry with a 53° end-to-end twist. In solution, variable-temperature ^{1}H NMR studies and molecular modeling present a story of rapid dynamic conformational interconversions between two C_2 enantiomers (with a low activation barrier) and a slower C_2-D_3 interconversion (with a relatively high barrier)—the first time clear evidence of conformational interchange for these hindered triphenylenes has been provided. Further studies have established that **5** is a fluorescent stable blue emitter, and that the compound undergoes an irreversible one-electron electrochemical oxidation. Calculations have predicted this to be a radical cation of C_2 geometry with 60° end-to-end twist.

Molecules that present functional groups in an atypical fashion, for example distorted from their preferred geometry, are intriguing targets for synthesis. Examples of systems previously examined include twisted amides[1] and nitro substituents[2] and the highly distorted aromatic rings found in several triphenylenes, naphthalenes, and pentacene cores.[3−7] These systems are inherently higher in energy than their non-strained cousins and can be far more reactive—the reactivity being driven by release of steric strain.[1,4] Overcrowded "D_{3h}"-symmetric[8] polycyclic aromatic hydrocarbons (PAHs) can adopt either a C_2 or D_3 (propeller-like) conformation.[9] The C_2 versus D_3 question is part of a wider issue regarding the driving forces underlying the conformational preference, i.e., sterics versus electronics, and considerable effort has been devoted toward resolving this point. Triphenylenes are a family that fit under the "D_{3h}" umbrella. Currently, only the moderately twisted peraryloxytriphenylene **1b**[10] and perfluorotriphenylene (**2**)[3,6] and the highly twisted perchlorotriphenylene (**3**)[4,5b] have been studied crystallographically, while aryloxy compounds **1a**,**c** and perbicyclo[2.2.2]octenetriphenylene (**4**)[11] have been synthesized but not characterized by X-ray.[12] However, Pascal et al. have suggested that halogen substituents may themselves have significant electronic effects which affect the structural characteristics.[9] As a result, they concluded that "the presently available experimental structures are perhaps not the very best examples for an examination of the C_2/D_3 dichotomy". They suggested and modeled four "ideal" candidates,[13,14] one of which was 1,4,5,8,9,12-hexamethyltriphenylene (**5**). They predicted that **5** would adopt a C_2 conformation, as opposed to D_3, with the C_2 system being computationally more stable by >7 kcal/mol. Therefore, the experimental realization of **5** would provide a model system for investigating many of the key issues, including conformational interconversions—an almost uncharted area of knowledge for these hindered triphenylenes. We report here the synthesis and complete characterization of compound **5**. This characterization includes X-ray crystallography, variable-temperature NMR (VT-NMR), molecular modeling, fluorescence spectroscopy, and cyclic voltammetry (CV).

(1) Tani, K.; Stoltz, B. M. *Nature* **2006**, *441*, 731−734.
(2) Hiyama, Y.; Brown, T. L. *J. Phys. Chem.* **1981**, *85*, 1698−1700.
(3) Hursthouse, M. B.; Smith, V. B.; Massey, A. G. *J. Fluor. Chem.* **1977**, *10*, 145−156.
(4) Shibata, K.; Kulkarni, A. A.; Ho, D. M.; Pascal, R. A., Jr. *J. Org. Chem.* **1995**, *60*, 428−434.
(5) (a) Pascal, R. A., Jr. *Chem. Rev.* **2006**, *106*, 4809−4819. (b) Shibata, K.; Kulkarni, A. A.; Ho, D. M.; Pascal, R. A., Jr. *J. Am. Chem. Soc.* **1994**, *116*, 5983−5984.
(6) Smith, V. B.; Massey, A. G. *Tetrahedron* **1969**, *25*, 5495−5501.
(7) (a) Lu, J.; Ho, D. M.; Vogelaar, N. J.; Kraml, C. M.; Pascal, R. A., Jr. *J. Am. Chem. Soc.* **2004**, *126*, 11168−11169. (b) Niemz, A.; Rotello, V. M. *Chem. Rev.* **1999**, *32*, 44−52. (c) Kroto, H. W. *Recent Res. Dev. Appl. Phys.* **2002**, *5*, 409−436. (d) Watson, M. D.; Fechtenkötter, A.; Müllen, K. *Chem. Rev.* **2001**, *101*, 1267−1300. (e) Wu, Y-T.; Siegel, J. S. *Chem. Rev.* **2006**, *106*, 4843−4867. (f) Tsefrikas, V. M.; Scott, L. T. *Chem. Rev.* **2006**, *106*, 4868−4884.
(8) The D_{3h} symmetry is related to how molecules are drawn on paper. Often, these structures are drawn without "wedged bonds", which is indicative of "D_{3h}" symmetry—this can be misleading.
(9) Barnett, L.; Ho, D. M.; Baldridge, K. K.; Pascal, R. A., Jr. *J. Am. Chem. Soc.* **1999**, *121*, 727−733.
(10) Frampton, C. S.; MacNicol, D. D.; Rowan, S. J. *J. Mol. Struct.* **1997**, *405*, 169−178.
(11) Nishinaga, T.; Inoue, R.; Matsuura, A.; Komatsu, K. *Org. Lett.* **2002**, *4*, 1435−1438.
(12) (a) Factual end-to-end twists: **1b**, 45.2°; **2**, 40.2°; **3**, 56.6°. Predicted (computed) twists: **4**, 61°; unsubstituted triphenylene, 2°. (b) A 1:1 co-crystal of perfluoro **2** and triphenylene gives corresponding twists of 33° and 16°. Weck, M.; Dunn, A. R.; Matsumoto, K.; Coates, G. W.; Lobkovsky, E. B.; Grubbs, R. H. *Angew. Chem., Int. Ed.* **1999**, *38*, 2741−2745.
(13) The experimental structures investigated were hexabenzotriphenylene, decacyclene, a hexa-*tert*-butyldecacyclene, perfluorotriphenylene (**1**), and perchlorotriphenylene (**2**). The three remaining theoretical structures examined, to the best of our knowledge, have not been synthesized. These are a hexamethyldecacyclene and two isomeric hexafurotriphenylenes.
(14) Peña, D.; Pérez, D.; Guitián, E.; Castedo, L. *Eur. J. Org. Chem.* **2003**, *7*, 1238−1243.

10.1021/ja074120j CCC: $37.00

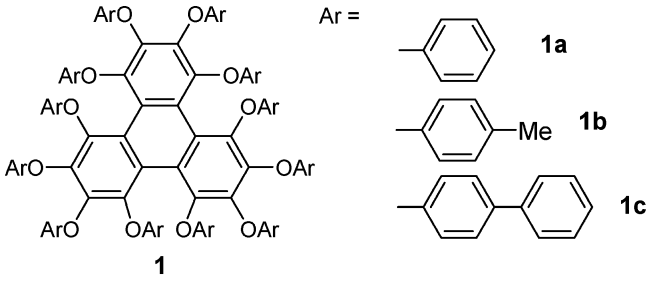

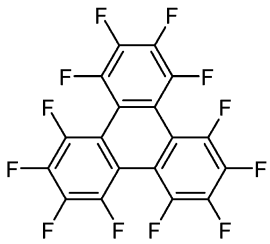

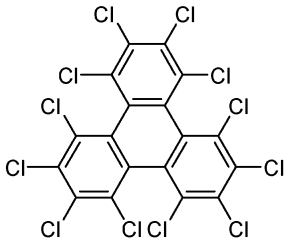

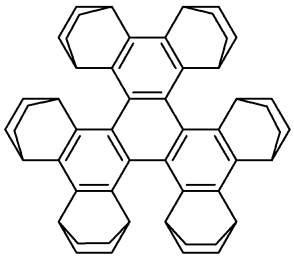

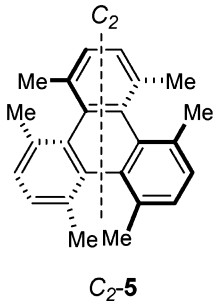

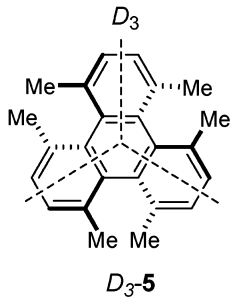

To prepare **5**, we exploited the fact that arynes undergo metal-catalyzed cyclotrimerization reactions to afford polycyclic aromatics (Scheme 1).[15−19] Treatment of commercially available 2,5-dimethylphenol (**6**) with *N*-bromosuccinimide (NBS; 15 °C) and hexamethyldisilazane (HMDS) afforded bromosilyl ether **7**. Sequential reactions with butyl lithium (BuLi) at −100 °C and triflic anhydride (−100 °C) provided the key *o*-trimethylsilylaryl triflate **8**. Then cesium fluoride was added in the presence of Pd catalyst to give **5** in 65% yield (33% overall).[20]

Examination of the NMR Traits of 5

The ^{1}H NMR spectrum of **5** at 25 °C (Figure 1) revealed only two sharp peaks, one aromatic singlet (7.18 ppm; 6H) and one methyl singlet (2.45 ppm; 18H). Initially, this was suggestive of D_3 symmetry, which was possible given the observations by Guitián et al. and Bennet et al. that the D_3 hexabenzotriphenylene product could be formed as the kinetic product[21] under similar mild reaction conditions. However, given Pascal's theoretical prediction that the C_2 conformer would be the thermodynamically most stable product, we decided to further characterize **5** using VT-NMR, X-ray crystallography, and computational modeling.

Scheme 1. Synthesis of 1,4,5,8,9,12-Hexamethyltriphenylene (**5**)[a]

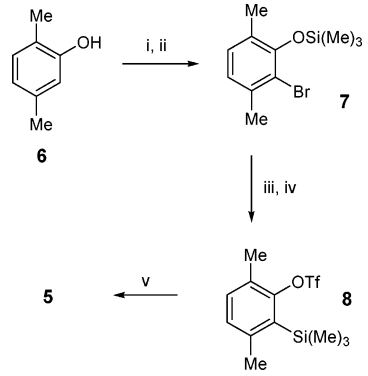

[a] Reagents and conditions: (i) NBS, 15 °C, 78%; (ii) HMDS, 80 °C; 98%; (iii) BuLi, −100 °C; (iv) Tf_2O, −100 °C, 66% (two steps); (v) CsF, $Pd(dba)_2$, 65%.

The results of the ^{1}H VT-NMR experiment are shown in Figure 1. On decreasing the temperature from 25 to −80 °C, the parent peak associated with the aromatic protons (7.18 ppm; 25 °C) resolved completely into two broad singlets (7.21 and 7.05 ppm; 4H and 2H, respectively; −80 °C), with partial resolution of the methyl singlet (2.45 ppm) into two overlapping broad peaks (2.41 and 2.35 ppm). From these data, a coalescence temperature (T_c) of −55 °C (220 K) was determined, which reveals rapid room-temperature conformational interconversions between two C_2 enantiomers rather than the presence of one D_3 conformer in solution. The activation energy (E_a) associated with this C_2-C_2 racemization was calculated using

$$E_a = \Delta G^{\ddagger} = RT_c[23 + \ln(T_c/\Delta\nu)]$$

where $T_c = 220$ K and $\Delta\nu = 57.6$ Hz. This gave $E_a = 10.20$ kcal/mol, which is a relatively low activation barrier, given the expected magnitude of methyl steric interactions. The rate of this interconversion, k, at T_c, was determined by using the formula

$$k = \pi\Delta\nu/\sqrt{2}$$

as 128 s^{-1}.[22] From the Arrhenius equation, assuming invariance of the frequency factor with temperature between T_c and

(15) Peña, D.; Pérez, D.; Guitián, E.; Castedo, L. *Org. Lett.* **1999**, *1*, 1555−1557.
(16) Peña, D.; Cobas, A.; Pérez, D.; Guitián, E. *Synthesis* **2002**, 1454−1458.
(17) Peña, D.; Escudero, S.; Guitián, D. P. E.; Castedo, L. *Angew. Chem., Int. Ed.* **1998**, *37*, 2659−2661.
(18) Peña, D.; Pérez, D.; Guitián, E.; Castedo, L. *J. Am. Chem. Soc.* **1999**, *121*, 5827−5828.
(19) Peña, D.; Pérez, D.; Guitián, E. *Angew. Chem., Int. Ed.* **2006**, *45*, 3579−3581.

(20) ^{1}H NMR (250 MHz, $CDCl_3$): $\delta = 7.18$ (s, 6H), 2.45 (s, 18H). ^{13}C NMR (62.5 MHz, $CDCl_3$): $\delta = 133.5$ (C, C-a), 131.4 (C, C-b), 129.3 (CH, C-c), 22.9 (CH_3, C-d). MS: $m/z = 312$ (M^+, 100), 154 (M − $C_{12}H_{12}$, 73), 77 (M − $C_{18}H_{19}$, 51). UV/vis (CH_2Cl_2): λ_{max} (ϵ_{max}) = 235 (12 500), 281 (23 200) nm (L mol^{-1} cm^{-1}). FT-IR (cm^{-1}): $\nu = 3044$, 2986, 2949, 2866, 1456, 1378. Elemental analysis, calculated: C, 92.24; H, 7.74. Actual: C, 92.26; H, 7.67. Mp = 160−162 °C.

(21) (a) Peña, D.; Pérez, D.; Guitián, E.; Castedo, L. *Org. Lett.* **1999**, *1*, 1555−1557. Peña, D.; Cobas, A.; Pérez, D.; Guitián, E.; Castedo, L. *Org. Lett.* **2000**, *2*, 1629−1632. (b) Bennett, M. A.; Kopp, M. R.; Wenger, E.; Willis, A. C. *J. Organomet. Chem.* **2003**, *667*, 8−15.

(22) The formula for determining rates is more commonly used for decoalesced peaks of equal intensity. However, the same formula can be applied to peaks of unsymmetrical intensities, as seen in our VT-NMR studies. Kost, D.; Carlson, E. H.; Raban, M. *Chem. Commun.* **1971**, *66*, 656−657.

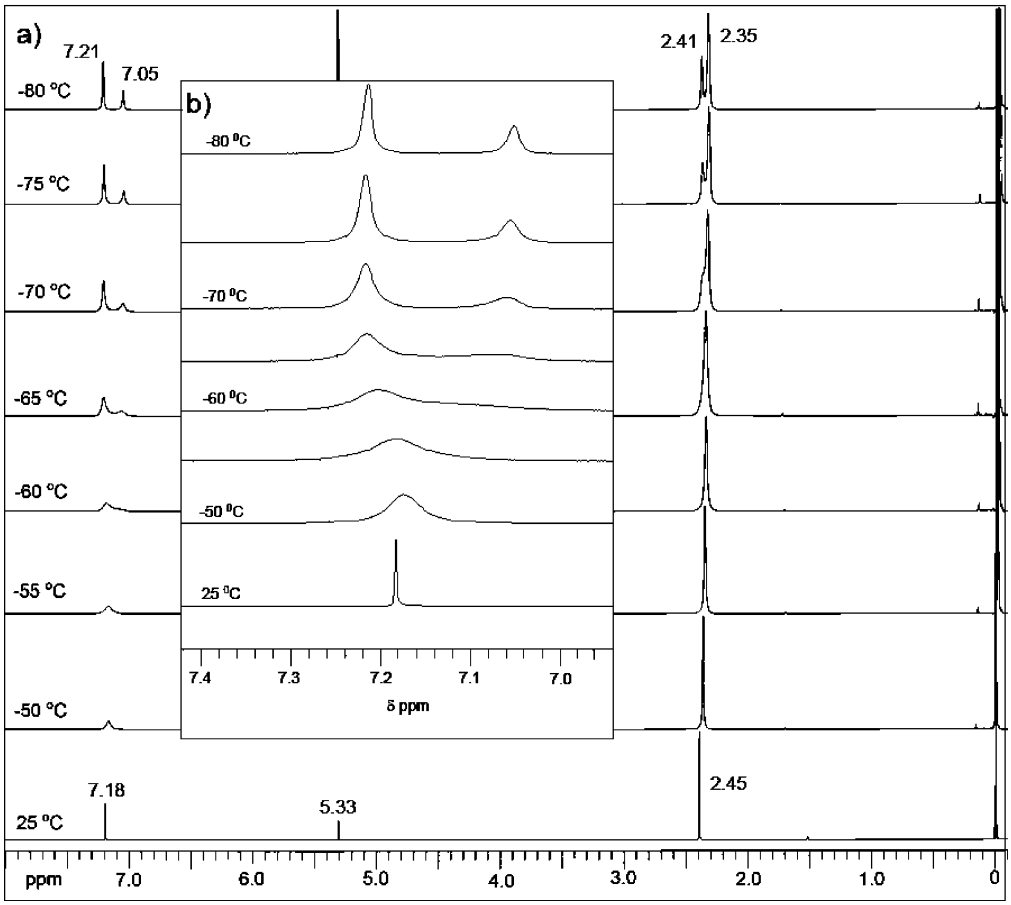

Figure 1. (a) ^{1}H VT-NMR spectra of **5** in 3:1 CS_2/CD_2Cl_2 (360 MHz). Temperatures ranged from 25 to −80 °C. The aromatic signal at 7.18 ppm (25 °C) resolved into two new signals, 7.21 and 7.05 ppm (−80 °C), and was concomitant with partial decoalescence of the methyl signal (2.45 ppm) into two overlying peaks, 2.41 and 2.35 ppm. ^{1}H NMR spectra were calibrated using TMS (0 ppm). Signal at 5.33 ppm is CH_2Cl_2. Note the "simple" NMR of **5** at 25 °C. (b) Inset showing scale-up of the aromatic region.

25 °C, this gives an estimate of k at 25 °C of 5.7×10^4 s^{-1}. This high interconversion rate explains the simple ^{1}H NMR spectrum that was observed at 25 °C.

It is interesting that only two distinct peaks were observed at low temperatures in the ^{1}H VT-NMR for the aromatic protons in Figure 1, rather than the three expected for this compound with C_2 symmetry. This is due to an accidental isochrony—two different types of protons with the same chemical shift (at 7.21 ppm at −80 °C). However, no accidental isochrony was observed in ^{13}C VT-NMR investigations at this temperature (see Supporting Information). In fact, the three aromatic peaks (132.900, 130.569, 128.771 (C−H) ppm) and one methyl peak (22.257 ppm) at 25 °C decoalesced into nine aromatic (133.997, 132.950, 132.731, 131.987 (C−H), 131.199, 130.143, 128.975, 128.836 (C−H), and 125.894 (C−H) ppm) and three methyl peaks (21.626, 22.734, 23.174 ppm) at −80 °C, respectively. This provides additional support for a C_2-symmetric conformation in solution.

X-ray Crystallographic Studies of 5

Unlike many other PAHs, compound **5** was found to be reasonably soluble in organic solvents. Colorless crystals suitable for X-ray studies were obtained by slow recrystallization of a saturated solution in ethanol. The X-ray structure of **5** is shown in Figure 2 in both framework and corresponding space-filled representations.[23,24] The crystal structure revealed a conformation similar to that of the highly twisted perchloro compound **3**; as a result, there are many parallels between the two systems. First, triphenylene **5** takes on a conformation with C_2 symmetry with very large deviation from planarity. This severe distortion enables alleviation of the "C:C" non-bonded contacts between adjacent methyl substituents. Even so, the average of nine non-bonded contacts in the crystal structure was 2.976 Å, well within the sum of the van der Waals radii of two carbons (3.4 Å), which indicates significant steric interaction. The $C_{Ar}-CH_3$ radial bonds of **5** are all similar in length (the six radial distances were 1.506, 1.513, 1.510, 1.507, 1.501, and 1.525 Å), with mean 1.510 Å. Second, rings B (C's 9−10−12−13−14−16) and C (C's 17−18−20−21−22−24) adopt boat conformations (Figure 2) with distortions approaching those of [8]paracyclophane.[5b] The remaining naphthalene substructure, rings A and D (C's 24−17−16−9−8−1−2−4−5−6), exhibits a 53° end-to-end twist, with the central ring A (C's 24−17−16−9−8−1) and ring D (C's 8−1−2−4−5−6) contributing 35° and 18°, respectively, to the overall twist. This value is similar to that for **3**, in which a 56.6° twist is present.[12] Third, strong bond

(23) (a) Altomare, A.; Cascarano, G.; Giacovazzo, G.; Guagliardi, A.; Burla, M. C.; Polidori, G.; Camalli, M. *J. Appl. Crystallogr.* **1994**, *27*, 435. (b) Betteridge, P. W.; Carruthers, J. R.; Cooper, R. I.; Prout, K.; Watkin, D. J. *J. Appl. Crystallogr.* **2003**, *36*, 1487. (c) Spek, A. J. *PLATON*; University of Utrecht: Utrecht, The Netherlands, 2006.

(24) (a) The crystal is a pseudo-merohedral twin. Parsons, S. *Acta Crystallogr., Sect. D: Biol. Crystallogr.* **2003**, *D59*, 1995−2003. (b) The crystal structure contains three crystallographically independent molecules. The majority of molecular crystal structures form with one molecule in the asymmetric unit. Steiner, T. *Acta Crystallogr.* **2000**, *B56*, 673−676.

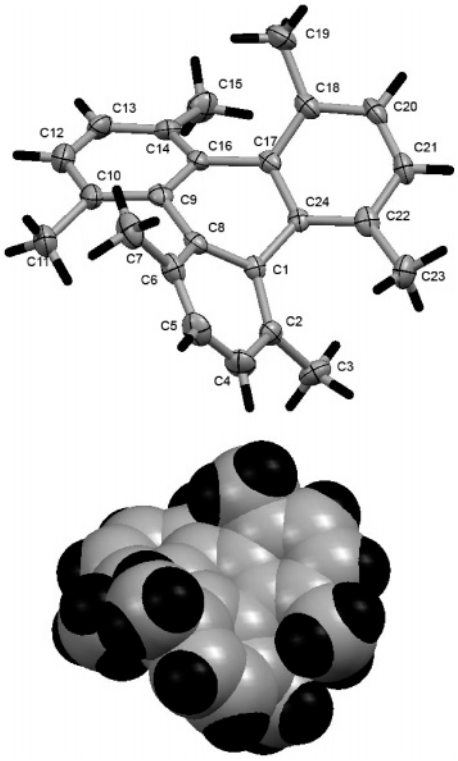

Figure 2. Molecular structure of **5** at 150 K (top) and the corresponding space-filled form (bottom). Hydrogen atoms shown in black. Thermal ellipsoids have been drawn at 50% probability.

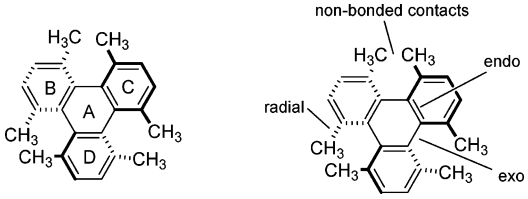

Figure 3. Structures showing ring labels and assignment of bond types for **5**. The wedge drawings correspond to the conformation present in the crystal structure in Figure 2. Mean bond lengths (Å): endo, 1.425; exo, 1.478; non-bonded contacts, 2.976; radial, 1.510.

alternation is seen in the central ring A (Figure 3). The endo bonds have mean length of 1.425 Å, while the exo bonds average 1.478 Å. The existence of bond alternation means that **5** can be regarded as three benzene rings (B, C, and D) linked together by bonds of low order. Indeed, it can be argued that it is the drive for "conservation of aromatization" in rings B, C, and D that induces such close C:C contact between the neighboring methyl groups. This seems to be a common trait in triphenylene compounds, such as triphenylene itself, peraryloxy **1b**, perfluoro **2**, and perchloro **3**. These properties lend significant weight to the argument that the geometries of these systems are governed by electronics and not sterics. Further evidence supporting this dictum is provided by the electrostatic potential maps of the C_2 and D_3 conformers of **5** (see Supporting Information).

At first glance, the experimental data seem to fit with Pascal's computational predictions[9] well. In particular, there are two aspects of the comparison that can be examined more closely. First, the circumference, which is measured as "3 exo + 3 endo bond lengths", arrived at from the computations can provide a good indicator of the actual conformation. It was stated that circumferences >8.6 Å would be associated with C_2 conformations. The predicted circumference was 8.72 Å, which matches well with the observed circumference of 8.71 Å and the resulting molecular shape. Second, it was anticipated that strong bond alternation in the central ring A would exist, typical of a C_2 conformer, and that exo and endo bonds with average lengths of 1.491 and 1.417 Å, respectively, would be seen. These values are reasonably close to the 1.478 (exo) and 1.425 Å (endo) bonds lengths observed for **5**. The difference appears to be due to an overestimation of the distortion by these HF/3-21G(*) computations. Non-bonded contact distances were unavailable and only low-level semiempirical (MNDO, AM1, PM3) and ab initio Hartree−Fock (STO-3G, 3-21G(*)) C_2 and D_3 ground-state computations without temperature correction were conducted by Pascal for hexamethyl **5**.[9] We therefore decided to use density functional theory (DFT) computational methods with enhanced basis sets, which were expected to be more accurate, to examine closely the ground states of the C_2-**5** and D_3-**5** conformers and the proposed transition states for C_2-C_2 racemization and C_2-D_3 interconversion at 298.15 K.

Molecular Modeling of Compound 5

Ground-state C_2 and D_3 structures were calculated using the Gaussian 03 program.[25] These stationary structures were confirmed as energy minima by means of vibrational analysis and the presence of zero imaginary vibrational frequencies. The geometries obtained were fully optimized both using a lower level ab initio HF/6-31G(d,p) calculation and an extended DFT B3LYP level using the basis sets 6-31G(d,p) and 6-311G-(d,p).[26−29] Concomitant with the ground-state studies, the transition states were initially located using semiempirical AM1 calculations implemented in Gaussian 03. These geometries were then fully optimized and confirmed as energy maxima using HF/6-31G and HF/6-31G(d,p), and B3LYP/6-31G(d,p) and B3LYP/6-311G(d,p), functionals and basis sets. The fully optimized structures for the C_2-**5** and D_3-**5** conformers, and the proposed transition states for C_2-C_2 racemization (**TS-I**) and C_2-D_3 interconversion (**TS-II**), are represented in Figure 4, together with the corresponding wedge structures, which demonstrate both the geometry and the symmetry of these systems. The relative disposition of the six methyl groups can be clearly seen.

The two transition states presented in Figure 4, **TS-I** and **TS-II**, are shown using the B3LYP/6-311G(d,p) method and basis set; they correspond to the C_2-C_2 and C_2-D_3 interconversions, respectively. Looking closely at these structures, it can be seen that **TS-I** presents "saddle-shaped" C_s symmetry, which results in a relatively low activation barrier, while **TS-II** is a more distorted C_2 system and is consistent with a considerably higher barrier to interconversion. The higher free energies calculated for the D_3 conformer (Table 1) explain the formation of the C_2 as the most stable thermodynamic product. To confirm that the C_2 conformer was thermodynamically most stable, we heated a

(25) Frisch, M. J.; et al. *Gaussian 03*, Revision C.02; Gaussian, Inc.: Wallingford, CT, 2004.
(26) The structures of all molecules were drawn using the visualization freeware ArgusLab. Thompson, M. A. ArgusLab 4.0.1; Planaria Software LLC: Seattle, WA, 2004 (http://www.arguslab.com).
(27) All calculations were run on the EaStCHEM research computing facility's Edinburgh computer cluster (http://www.eastchem.ac.uk/rcf).
(28) Output was viewed using the Gabedit visualization software, freely available from the Internet (http://gabedit.sourceforge.net/).
(29) Images (Figure 4) were rendered using the Persistence of Vision Raytracer (POV-Ray) freeware (http://www.povray.org).

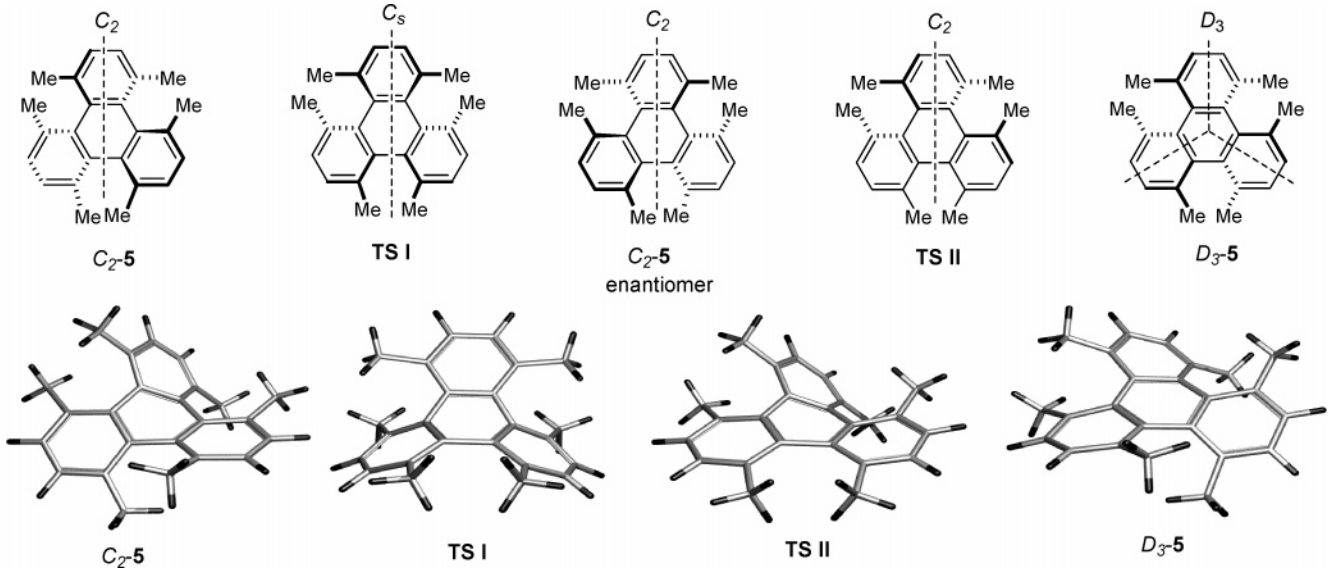

Figure 4. Schematic drawings of the C_2 and D_3 conformations and the transition states of hexamethyltriphenylene **5** (top). Corresponding optimized molecular geometries for the B3LYP/6-311G(d,p) functional and basis set (bottom).

Table 1. Temperature-Corrected Calculated Free Energies of Ground States and Barriers to Conformational Interconversions (Activation Energies) in kcal/mol at 298.15 K Relative to the C_2 Ground State

method	D_3 conformer	C_2–C_2 **TS-I**[a]	C_2–D_3 **TS-II**
AM1	+1.41	+7.84	+23.98
HF/6-31G	+6.44	+11.11	+30.40
HF/6-31G(d,p)	+5.91	+10.93	+29.42
B3LYP/6-31G(d,p)	+4.97	+9.80	+25.42
B3LYP/6-311G(d,p)	+4.97	+9.64	+25.47

[a] Exptl: 10.20 kcal/mol.

small quantity of hexamethyltriphenylene **5** in DMSO-d_6 at 170 °C for 6 h. A carefully calibrated ^{1}H NMR verified no change in the spectrum. It is interesting that this synthetic method has always previously given the C_2 conformation as the initially formed product, even when this is not the most thermodynamically stable—as seen for the formation of the kinetic C_2 hexabenzotriphenylene product.[21] The formation of the thermodynamic product suggests that these synthesis conditions favor the formation of a molecule with C_2 symmetry, perhaps because the reaction components come together in such a way that the transition state closely resembles the C_2 rather than D_3 structure.

Some deviation in the quantitative data in Table 1 is clearly seen, as a result of the differing levels of theory employed for the calculations. Semiempirical AM1 has been shown to be fairly effective at modeling similar barriers observed in hexabenzotriphenylene[21a] but underestimated the C_2-C_2 barrier of **5**, as is shown by this temperature-corrected data. Ab initio Hartree−Fock calculations are known to overestimate energy barriers to conformational interchange and, as expected, give greater values for both C_2-C_2 and C_2-D_3 conformational interchanges than the other methods. The variation of these Hartree−Fock barriers could be the result of neglecting electron correlation effects, which are anticipated to be significant for the conformational interconversions that proceed via greatly distorted transition states.[21a] The best agreement between the calculated and experimental activation energies (within 0.4−0.6 kcal/mol) was achieved by using DFT calculations using the B3LYP functional with two basis sets, 6-31G(d,p) and 6-311G(d,p), consistent with the fact that DFT takes into account electron correlation effects. Such differences are small and may be due to the effects of solvation (not considered in these calculations). All calculated C_2-D_3 energy barriers were similar and significantly higher than the C_2-C_2 barriers.

To ascertain the degree of fit between the computed C_2 ground-state structures and the X-ray structure, root-mean-square deviations (rmsd's)[30] were calculated using the Visual Molecular Dynamics (VMD 1.8.5) program.[31] These analyses revealed that all the carbon skeletons of the modeled geometries matched the corresponding backbone of the X-ray structures very well (rmsd range 0.028−0.056), although some discrepancies were observed. As expected, the B3LYP/6-31G(d,p) and B3LYP/6-311G(d,p) produced C_2 conformers with the best fit (mean 0.040 and 0.042, respectively). Furthermore, the non-bonded contacts were best handled by these DFT methods; the average distance for nine contacts in the crystal[32] was 2.976 Å, while averages of 2.996 (6-31G(d,p)) and 3.003 Å (6-311G(d,p)) were observed for the DFT structures. The HF/6-31G and HF/6-31G(d,p) geometries (mean 0.045 and 0.047, respectively) showed greater deviation when compared to the DFT methods, which may be due to the lack of electron correlation effects in the calculations.[21a] However, the non-bonded contacts—3.000 (6-31G) and 3.005 Å (6-31G(d,p))—were reasonably close to the experimental value. The AM1 conformer (mean 0.045) seemed to provide a match to the crystal data similar, overall, to HF; however, the non-bonded contacts (2.908 Å) were grossly underestimated—a problem that has been observed prior to this study.[9] The exo (1.478 Å) and endo (1.425 Å) bonds lengths, seen in the crystal structure, were matched best utilizing the B3LYP/6-31G(d,p) and B3LYP/6-311G(d,p) functionals and basis sets. These gave corresponding mean lengths of 1.481 (exo) and 1.433 Å (endo) and 1.479 (exo) and 1.431 Å (endo), respectively. Both of these

(30) Due to the presence of poorly diffracting hydrogen atoms, only the carbon backbones were compared.
(31) Humphrey, W.; Dalke, A.; Schulten, K. *J. Mol. Graphics* **1996**, *14*, 33−38. The VMD 1.8.5 program is available from the Internet (http://www.ks.uiuc.edu/Research/vmd/).
(32) All nine distances (Å): 3.007, 2.938, 2.967, 3.005, 2.985, 2.941, 2.955, 2.954, and 3.030.

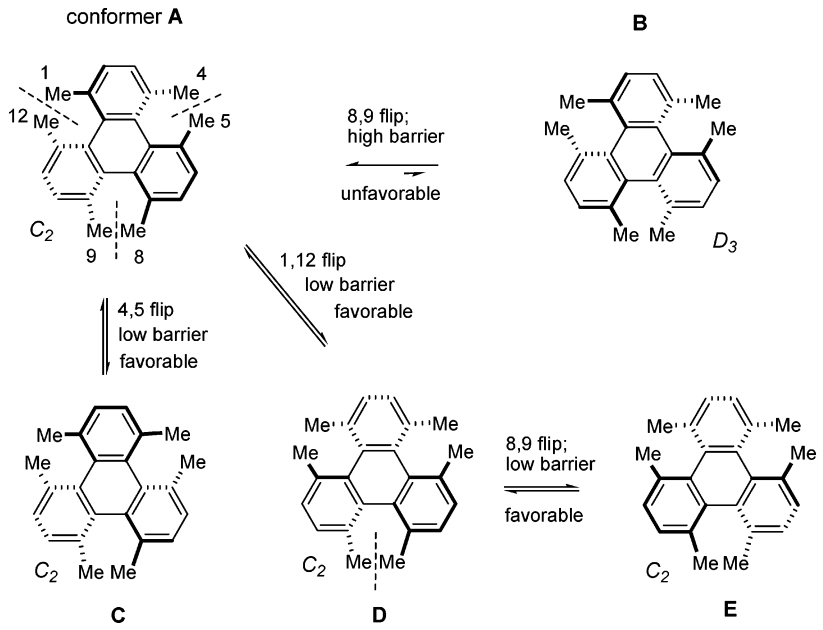

Figure 5. Wedge drawings of **5**, illustrating the rapid conformational interconversions that provide averaged ^{1}H NMR signals. Computations indicate that the mechanism proceeds chiefly through successive low-barrier C_2-C_2 interchanges.

methods afforded extremely good fits and show the value of employing DFT calculations for these systems. The HF and AM1 methods gave poorer fits, both underestimating the degree of distortion.

All calculations in Table 1 demonstrated that the C_2-D_3 energy barrier is substantially higher than the one for the C_2-C_2 interconversion. An interesting upshot of this high barrier is the implication that methyl flipping, between neighboring methyl substituents, mostly occurs when the resulting conformer is C_2, not D_3. By analyzing the conformational dynamics, a complete picture for **5** is provided (Figure 5). Conformer **A** has three possible sites for flipping: the neighboring methyl substituents at the 1,12, the 4,5, and the 8,9 positions. First, flipping of the 8,9-methyl groups affords **B**, which is a D_3 system, so it is unfavorable. Second, the 4,5-methyl interchange is favorable, as it provides **C**, which presents C_2 symmetry. Third, the 1,-12-exchange is also favorable, providing the C_2 conformer **D**. If this exchange is followed by an 8,9-flip, conformer **E** with C_2 symmetry results, meaning that the 8,9-flip is now favorable (cf. **A** to **B**). In a short time, all the methyl groups are rapidly scrambled ($k = 5.7 \times 10^4$ s^{-1}), with the flipping mechanism proceeding mainly through low-energy C_s transition states; rapid flipping manifests itself as single sharp peaks in the NMR spectrum (Figure 1a).

Conformational Analyses of Hindered Triphenylenes 1−4

This is the first time that solid evidence has been provided for the dynamic conformational interconversion mechanism for this class of hindered triphenylenes. Pascal's group was the first research group to propose possible dynamic exchange between two enantiomers after synthesizing perchloro **3**.[4] Low-level AM1 calculations of this system were conducted after failing to resolve the enantiomers by conventional means, and they hinted at the possible existence of racemization that progressed via a low-energy barrier—where the calculated C_2-C_2 and C_2-D_3 barriers were 7.0 and 26.1 kcal/mol, respectively. However, due to the physicochemical makeup of **3**, it is not possible to validate this. Perfluorotriphenylene (**2**), unlike **3**, does have useful NMR active nuclei for investigating the conformational dynamics in solution. ^{19}F NMR was performed only at 25 and −40 °C, with the conclusion that "a propeller-like distortion (D_3) must exist in solution",[3,6] even though a C_2 structure was observed in the crystal (the thermodynamic product), and there was no suggestion of conformational interchange. Since we believe an incomplete picture for **2** persists, we performed AM1 and B3LYP/6-311G(d,p) computational studies on this molecule. Similar to our system, perfluorotriphenylene **2** can undergo dynamic conformational interchange, although with a slightly different mechanism. The 6-311G(d,p) C_2-C_2 and C_2-D_3 barriers—1.96 and 6.57 kcal/mol, respectively—are *both* low.[33] As a consequence, both the C_2-C_2 racemization and C_2-D_3 interconversions can occur very rapidly and easily at room temperature, which gives rise to the appearance of a sharp averaged "D_3" NMR signal in solution, even at −40 °C. Neither the peraryloxytriphenylenes **1a−c** nor perbicyclo[2.2.2]-octenetriphenylene (**4**) was investigated for any type of conformational interchange, as no low-temperature NMR studies were reported. However, we anticipate that dynamic conformational interconversions do occur for all these systems, although to varying degrees. For aryloxy compound **1b**, the C−O *inner* bond length is 1.377 Å and the van der Waals radius for oxygen is 1.4 Å.[10] Given that these are slightly longer and larger than the corresponding values for the C−F bonds of **2** (1.330 Å; vdW radius $F = 1.35$ Å), it then seems reasonable to imagine that dynamic conformational interchange is present and occurs rapidly at room temperature, at a rate somewhere between those observed for **2** and **5**. Supporting evidence is provided by the low-level AM1 calculation on a *mimic* of **4**, which suggests that the C_2-C_2 barrier is approximately 6.08 kcal/mol.[34,35] For peroctene **4**, the steric demands are expected to be greater than those for perchloro **3** and hexamethyl **5**, since molecular modeling studies predicted a 61° twist, although this

(33) The AM1 barriers were 0.82 and 3.45 kcal/mol for the C_2-C_2 and C_2-D_3 barriers, respectively.

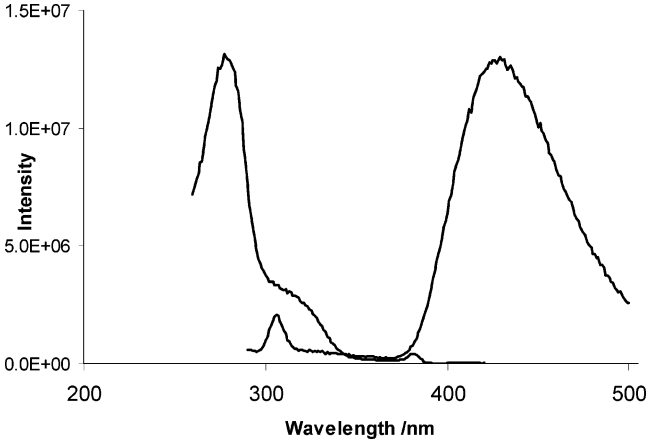

Figure 6. Excitation (at the peak emission wavelength, $\lambda_{em} = 430$ nm, left) and emission (at the peak excitation wavelength $\lambda_{ex} = 280$ nm, right) spectra for **5**. [**5**] $= 1 \times 10^{-6}$ M in ethanol. Quantum yield (φ_F) was 7% when measured with comparison to indole ($\varphi_F = 0.4$). The emission peak seen near 310 nm and excitation peak near 380 nm are both solvent Raman bands. The quantum yield was estimated by making a comparative measurement using indole as standard, which has a known quantum yield of 40% in ethanol solution.[36] Low ($\sim\mu$M) comparable concentrations of sample and standard were used to ensure that inner filter effects were negligible. For both sample and standard, the quantum efficiency is proportional to the ratio of the integrated emission intensity (the area under the measured emission spectrum) to the integrated absorption intensity (the area under the measured absorption spectrum).

not been verified by X-ray characterization. If correct, this implies that that any conformational interconversions are likely to proceed in a manner mechanistically similar to those for **3** and **5**, although with higher activation barriers. A C_2-C_2 transition state was located at the AM1 level and produced a barrier of 7.33 kcal/mol.[35] Surprisingly, this was very close to the barrier provided for **3** and **5**, indicating rapid interconversion at room temperature.

Fluorescence Spectroscopy of 5

Steady-state fluorescence spectroscopy showed that hexamethyltriphenylene (**5**) is fluorescent, emitting light in the blue region of the spectrum (Figure 6). Currently, the study of this class of compounds is highly desirable due to their potential applications in optoelectronics, such as in organic light-emitting diodes (OLED).[37] A large Stokes shift ($\Delta\lambda = 110$ nm) between the first absorption maximum ($\lambda_{max} = 320$ nm) and the emission maximum ($\lambda_{max} = 430$ nm) was observed. This is consistent with a relatively large change in molecular configuration upon excitation. This is expected, as excitation should involve a $\pi-\pi^*$ electronic transition, resulting in a decrease in π-bonding and an increase in the importance of steric repulsion. The quantum yield for fluorescence (φ_F) of **5** was measured as 7% at room temperature. These spectral characteristics are comparable to those reported for a dibenzotriphenylene derivative previously studied, which also gives blue fluorescence and a similar quantum yield.[38]

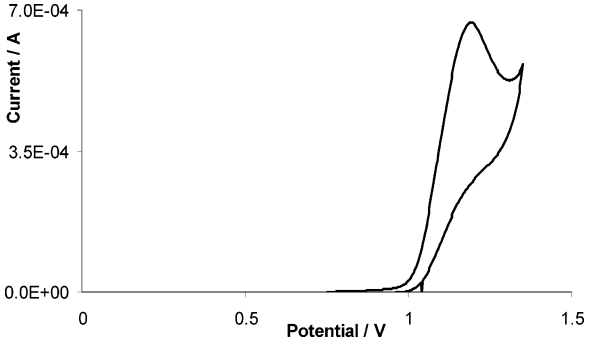

Figure 7. Cyclic voltammogram of **5**. [**5**] = 1 mM in background electrolyte solution of 0.1 M anhydrous $LiClO_4$ in acetonitrile (dried; distilled). The reference electrode was made in-house and consists of a Ag wire dipped into a solution of $AgClO_4$ (0.01 M) in background electrolyte solution, with a measured potential of −0.074 V vs the Fc/Fc^+ couple. The counter electrode was a 2 cm^2 Pt gauze, and the working electrode was a 0.387 cm^2 Pt rotating disc electrode. These were controlled by an AUTOLAB PGSTAT30 potentiostat (Eco Chemie BV) equipped with GPES 4.9 software.

Electrochemical Investigation of 5

Cyclic voltammetric (CV) analysis of hexamethyltriphenylene (**5**; Figure 7) showed an irreversible one-electron oxidation wave ($E_{pa} = 1.10$ V vs Fc/Fc^+) at all sweep rates studied between 20 and 500 mV/s. This behavior is analogous to the previously observed irreversible one-electron oxidation of the unsubstituted triphenylene ($E_{pa} = 1.50$ V in benzonitrile vs Fc/Fc^+).[11] As might be expected, consistent with the electron-donating nature of the six methyl substituents, the oxidation peak of **5** was intermediate between those of unsubstituted triphenylene and peroctenetriphenylene (**4**), where **4** exhibited a reversible one-electron oxidation wave ($E_{1/2} = 0.44$ V vs Fc/Fc^+). Komatsu et al.[11] stated that the dramatically decreased oxidation potential of **4** was due to the intrinsic electronic effects of annelation with the bicyclo units, which raise the HOMO level of the π-system through the inductive electron donation and $\sigma-\pi$ interactions, coupled with the additional elevation of the HOMO resulting from the large deviation from planarity. It is possible that the electrochemical reversibility of **4** may be due to the very bulky nature of the bicyclo units, which provide a "protective shell" (akin to site isolation) surrounding the oxidized species, preventing it from showing the enhanced reactivity usually seen in these strained systems by undergoing further chemical reaction to form redox-inactive species. This would not be the case for **5** and triphenylene, for which rearrangement and/or intramolecular coupling reactions are likely. For this reason, it would be intriguing to synthesize and electrochemically characterize a permethylated triphenylene, which would be completely peripherally protected against intramolecular coupling through complete functionalization with 12 methyl substituents.

Calculations of the temperature-corrected free energies of **5** and the one-electron oxidation product $\mathbf{5}^{+\bullet}$, each with C_2 symmetry, along with those for indole (In) and the one-electron oxidation product of indole ($In^{+\bullet}$), were carried out using B3LYP/6-311G(d,p) at 298.15 K in acetonitrile, using the polarizable continuum model.[39] This resulted in a calculated oxidation potential of **5** of +1.11 V vs Ag/Ag^+ (0.01 M),

(34) Due to the size and complexity of peraryloxytriphenylene (**1b**), a mimic was employed in the modeling calculations. Six phenyl groups were replaced with methyls at the 2, 3, 6, 7, 10, and 11 positions. However, only the 1, 4, 5, 8, 9, and 12 positions are involved in the distortions and were left unchanged. A complete structure of the mimic can be seen in the Supporting Information.
(35) We assume that the underestimation that occurs for the AM1 barriers for hexamethyl **5** also occurs for **1b** and **4**.
(36) Kirby, E. P.; Steiner, R. F. *J. Phys. Chem.* **1970**, *74*, 4480.
(37) Xu, Q.; Duong, H. M.; Wudl, F.; Yang, Y. *Appl. Phys. Lett.* **2004**, *85*, 3357−3359.
(38) Morrison, D. J.; Trefz, T. K.; Piers, W. E.; McDonald, R.; Parvez, M. *J. Org. Chem.* **2005**, *70*, 5309−5312.

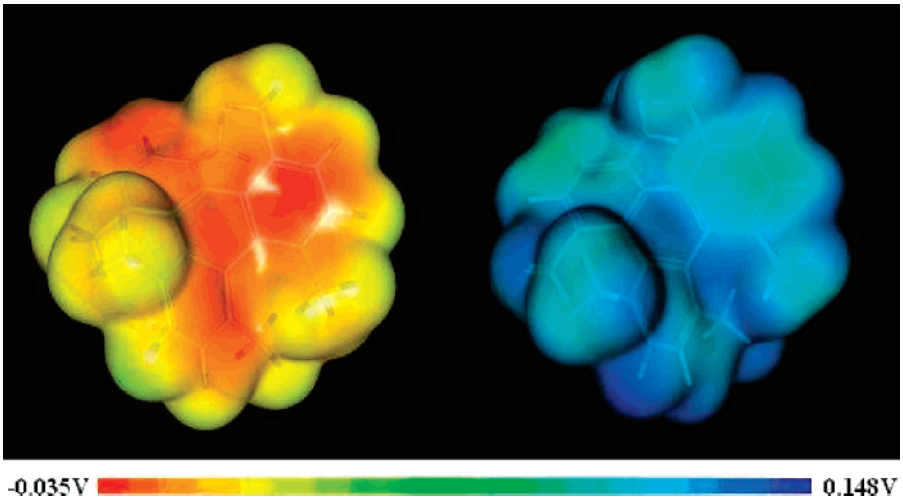

Figure 8. Electrostatic potential maps for the optimized geometries of **5** and $\mathbf{5}^{+\bullet}$. Red is electron-rich, blue is electron-poor. As well as the overall decrease in electron density upon oxidation (an overall shift in color from red to blue), the potential map for $\mathbf{5}^{+\bullet}$ also reveals the decrease in π-bonding and delocalization after oxidation—a blue electron-poor region is clearly seen where ring D is joined to ring A.

compared with the experimentally observed value of +1.14 V. Given that equivalent calculations showed D_3-$\mathbf{5}^{+\bullet}$ to be of significantly higher energy than C_2-$\mathbf{5}^{+\bullet}$, this good agreement between experimental and calculated oxidation potentials supports the formation of the more thermodynamically stable C_2-$\mathbf{5}^{+\bullet}$ as the oxidation product.

The calculated structure of C_2-$\mathbf{5}^{+\bullet}$ (Figure 8) shows an increased twist in the naphthalene substructure, with rings A and D (C's 24−17−16−9−8−1−2−4−5−6) exhibiting a 60° end-to-end twist. This is consistent with the calculated increase in the methyl separations (C's 3−23 and C's 7−11) from 2.99 to 3.02 Å and can be attributed to an increase in the importance of steric repulsion due to the reduction in aromaticity brought about by removal of a π-electron. This increased twist also appears to affect electronic delocalization (Figure 8). In **5**, electron density can be seen to be distributed across the entire aromatic system. However, on oxidation, a region of lower electron density (darker blue) can be seen where ring D joins ring A (Figure 2), along with a region of higher electron density (green area) in rings B and C. Significant bond lengthening is also found in four of the six C−C bonds in ring D (see Supporting Information). This is consistent with the increased twist in ring D decreasing π-bonding and electronic delocalization in and around this ring.

In summary, the model compound 1,4,5,8,9,12-hexamethyltriphenylene (**5**) has been prepared for the first time. X-ray studies have revealed a highly distorted C_2 structure with a 53° end-to-end twist. We have shown through experiment and computation that **5** displays dynamic conformational interchange in solution, and we have provided computational evidence that this phenomenon is active in all hindered triphenylene systems. We have also shown it to be fluorescent in the blue and electroactive, as well as possessing good solvent solubility and electroactivity. Fluorescence, electrochemical measurements, and calculations have shown that both the excited-state and oxidized forms of **5** show significant differences in geometry, consistent with the decrease in π-bonding brought about by excitation and by oxidation, which increases the end-to-end twist to 60°.

Acknowledgment. We thank the Royal Society for a University Research Fellowship (T.H.G.) and the University of Edinburgh for Ph.D. studentships (A.D.S. and J.B.H.). This work has made use of the resources provided by the EaSTCHEM Research Computing Facility (http://www.eastchem.ac.uk/rcf). This facility is partially supported by the eDIKT initiative (http://www.edikt.org). We are also grateful to David A. Leigh, Andrew Turner, Herbert Fruchtl, Ian Sadler, Anita Jones, and John Miller for helpful discussions.

Supporting Information Available: Full descriptions for the synthesis of **5**, including ^{1}H and ^{13}C NMR, MS, UV, and FT-IR spectra; X-ray characterization material, including data collection and crystal parameters, atomic coordinates, anisotropic displacement coefficients, bond lengths and bond angles, and least-squares planes; a second cyclic voltammogram, and an image of **5** fluorescing; electrostatic potential maps of C_2 and D_3 conformers; rmsd table and calculated bond lengths for and differences between **5** and $\mathbf{5}^{+\bullet}$; "absolute energies" and optimized geometries (as Cartesian coordinates) for all calculated structures; and complete ref 25. This material is available free of charge via the Internet at http://pubs.acs.org.

JA074120J

(39) It has previously been shown that accurate calculation of absolute values of experimental indole oxidation potentials is possible to within a few tens of millivolts, making this suitable as a reference redox reaction. Calculation of the free energy of the reaction $\mathbf{5}^{+\bullet} + \mathrm{In} \rightarrow \mathbf{5} + \mathrm{In}^{+\bullet}$ gives the oxidation potential of **5** relative to In. This can then be converted to a calculated oxidation potential on any reference scale by using the experimentally measured value of the indole oxidation potential. Experimental oxidation potentials are obtained from the measured peak potentials, E_p, as $E_p - E_{1/2} = 28.5$ mV for a reversible one-electron redox reaction at 298 K, and the half-wave potential $E_{1/2}$ can be considered equal to the standard redox potential (the oxidation potential) when reactants and products have similar diffusion coefficients in solution. Kettle, L. J.; Bates, S. P.; Mount, A. R. *Phys. Chem. Chem. Phys.* **2000**, *2*, 195−201.